Available online at www.elixirpublishers.com (Elixir International Journal)

Dye Chemistry

Elixir Dye Chem. 56 (2013) 13510-13518

ISSN: 2229-712X

# The influence of the oxidizing agents on the rates of degradation of Rose bengal using Titanium oxide nanoparticles

C.Mathivathana[1], V. Balasubramanian[1,*] and K.Pandian[2]

[1]Department of Chemistry, AMET University, Kanathur, Chennai-603112, India.

[2]Department of Inorganic Chemistry, University of Madras, Chennai-600025, India.

**ARTICLE INFO**

**Article history:**

Received: 22 January 2013;

Received in revised form:

11 March 2013;

Accepted: 15 March 2013;

**Keywords**

Rosebengal,

Degussa P-25,

Nano $TiO_2$,

Fenton reagent,

Photo Fenton process.

**ABSTRACT**

Uniform sized$TiO_2$ nanoparticleswere synthesized using the sol-gel method, and the resultant powdered $TiO_2$ samples was heated at 500°C air atmosphere. Samples characterized by the XRD, FTIR, TGA and SEM and the photocatalytic degradation of Rose bengal using $TiO_2$ nanoparticles havebeen tested under UV light irradiation at 352nm (Long Wavelength). The rate of degradation of Rose bengalwas monitored by measuring the decrease in the absorbance value. Experimental parameters, such as the amount of catalyst loading, dye and $H_2O_2$ concentrations and Fenton's reagent was tested against the degradation rate. The degradation efficiency of the synthesized nanoparticles was tested against commercially available $TiO_2$ (Degussa P-25).

© 2013 Elixir All rights reserved.

## 1. Introduction

Dyes are widely used in textile, leather, paper, printing inks, plastics, cosmetics, paints, pharmaceutical, and food industries. In 2008, the World's colorant production was about 1.5million tones [1].Being a common industrial pollutant, there has been a necessity for the decolourisation and mineralization of the dyes, using various methods.

The application of conventional biologicaltreatment methods for the decolourisationof organic dye has been ineffective due to the presence of aromatics[2-7]. Alternatively,photocatalytic technology gained much attention on degrading organic pollutants completely from waste water [8-11].Many attempts have been made tostudy the photocatalytic activity of different semiconductors such as $SnO_2$, $ZrO_2$, CdS, ZnO [12-16]. However, ZnO and CdS arephoto corrosive and lose their catalytic activity on prolonged usage. CdS are less active compared to $TiO_2$. The band gap in $WO_3$ (band gap = 2.76 eV) is less than in $TiO_2$. Though $ZrO_2$ is a stable and non-photo corrosive photocatalyst, its band gap is around 4 eV. Hence, it is less active compared to other photocatalyst. Among all these semiconductors, the most widely used semiconductor catalyst in photo induced processes is titanium dioxide ($TiO_2$). Due to this,$TiO_2$, a heterogeneous photocatalyst has been considered asa more attractive compound, due to its free availability, inexpensiveness, non-toxicity and its potential, physical and chemical properties [17,18]. It is well known that there are three crystalline forms of $TiO_2$: Brookite, Anatase and Rutile. Among these, the Rutile phase is the most thermodynamically stable one, compared to Brookite and Anatase, which are metastable and get transformed to rutile on heating [19]. In order to enhance the photocatalytic behaviour, titanium oxide doped with metals and non-metals has been widely used. Though $TiO_2$ has its advantages, it has its own limitations of therapid recombination rate of the photo generated electrons, and holes in the $TiO_2$, resulting to low quantum efficiency. This has led to an urgent need to develop an efficient method ofproducing photocatalytic materials. To have an enhanced oxidation process regenerating fresh surface, we tried adopting a photocatalytic degradation method, by combining the photocatalytic system with anAdvanced Oxidation Process (PhotoFenton reagents).

Fenton reagent [20], a mixture of hydrogen peroxide and ferrous salt, is a powerful oxidant for many organic compounds, and has attracted interest in wastewater treatment [21-23]. The success of Fenton reagent for the oxidation of a variety of organic contaminants is attributed to the generation of hydroxyl radicals, formed during the catalytic decomposition of hydrogen peroxide in acidic media. The hydroxyl radical is generated according to the following reaction [24-26].

$$Fe^{2+} + H_2O_2 \rightarrow Fe^{3+} + HO^- + \bullet OH \qquad (1)$$

Besides the high efficiency of the reaction, iron is a non-toxic element and can be separated from treated wastewater by coagulation, while $H_2O_2$ is easy to handle, environmentally safe and is consumed during the usual degradation process. The addition of organic oxidants such as $ClO^{2-}$, $ClO^{3-}$, $BrO^{3-}$, $H_2O_2$, $IO^{4-}$and $S_2O_8^{2-}$to the $TiO_2$ photocatalyst has been investigated with and without the presence of inorganic oxidants [27, 28]. The presence of Fenton's reagent in the reaction mixture plays a key role in the photocatalytic degradation of the dyes [29-31]. The degradation of organic pollutants by the Fenton reagent can be significantly accelerated in the presence of UV irradiation, resulting in the complete mineralization of organic pollutants known as PhotoFenton process.

The purpose of the present study is to evaluate the efficiency of the PhotoFenton process for the decolourization and Photodegradation of the Rose bengal. The efficiency of degradation was compared with that of UV/Degussa P25, UV/nano $TiO_2$ and by Photo Fenton process. The PhotoFenton

Tele:

E-mail addresses: baluiisc80@gmail.com

© 2013 Elixir All rights reserved

reaction under UV irradiation was studied, with the aim to propose a low cost alternative for the treatment of wastewater dye contamination, becoming more attractive for industrial applications. The effects of the key operating parameters, such as catalyst loading, Fenton reagent concentration as well as the influence of the initial dye concentration on the decolourization and mineralization extent were also studied.

## 2. Experimental

### 2.1. Material and Methods

All the reagents used were of an analytical grade. The commercial samples of Rose bengal(4, 5, 6, 7-tetrachloro-2', 4', 5', 7'-tetraiodofluorescein) were supplied by Vanavil (India) Ltd, and those of the photocatalyst $TiO_2$ were supplied by Degussa Co., Germany. Nano $TiO_2$ (synthesized in the lab) and the ferrous ions from solutions of $FeSO_4.7H_2O$, ethyl alcohol, $H_2O_2$ were obtained from Merck (30% w/w).

In the photo bleaching process, Rosebengal ($1.0\times10^{-3}$ M solution) and $FeSO_4$ ($1\times10^{-3}$ M) are prepared in a volumetric flask with double distilled water, and stored as a stock solution. The pH of the solution is adjusted by the $H_2SO_4$ and NaOH solutions. The reaction mixture was prepared by diluting the stock solution to the desired level, with all the three catalysts of varying concentrations. The photocatalytic degradation study was carried out in a batch reactor of 200 ml capacity as the outer jacket, and a UV lamp (354 nm) placed inside the quartz tube. The reactor was placed on a magnetic stirring plate to enhance the agitation. After specific intervals of irradiation, the samples were withdrawn and analyzed after centrifugation. The decolourisations of the sample were observed by measuring the absorbance, using the UV-Vis spectrophotometer (Shimadzu UV-1601 model, Japan). A blank experiment of $5\times10^{-6}$ M was done to find out the time taken for the completion of decolourisation, and a higher concentration was prepared using Fenton's reagent to stabilize the amount of $FeSO_4$ and $H_2O_2$ solution to be used for the photodegradation.

### 2.2. Preparation of $TiO_2$ Nanoparticles

$TiO_2$ (Anatase phase) nano powders were prepared via the sol-gel method [32, 33] using Titanium tetra-isopropoxide (TTIP, Sigma Aldrich). The concentrations of the TTIP; EtOH; $H_2O$; HCl were in the ratio of 1:15:60:2. The TTIP was dropped slowly in the solution of $H_2O$, alcohol and acid, while magnetic agitation was done continuously to get a white precipitate. The obtained solutions were kept under constant stirring on a magnetic stirrer for 48 h at room temperature. Then the precipitate was filtered and dried at 150 $^oC$ for 2 h, until it turned into a white block crystal. After the ball milling, the dried powders obtained were calcined at 500 $^oC$ for 3h to observe the phase change accompanying the heat treatments.

## 3. Results and Discussion

### 3. 1. FT – IR spectral studies for Nano Titania

FT-IR spectra of the prepared and calcined samples of $TiO_2$ are represented in Fig 1(a),and it shows the narrow bands in the range of 3600-2800 $cm^{-1}$,and the maximum of 3355$cm^{-1}$ arises from the position of the interacting hydroxyl groups of the organic solvents. The stretching vibrations of the $–CH_2$ and –CH bands at 2968, 2929, 2897, 2498, 1482 and 1250 $cm^{-1}$ are attributed to the organic residues which originate from the preparation route. In Fig1(b)$TiO_2$ calcined at 400$^oC$ reveals a minor change in vibration frequencies, and the removal of most of the weakly adsorbed interacting organic impurities and the hydroxyl groups. In Fig 1(c), the $TiO_2$(calcined at 500$^oC$) the peak noticed at 500$cm^{-1}$ may be attributed to the formation of a structure containing the Ti-O linkage.

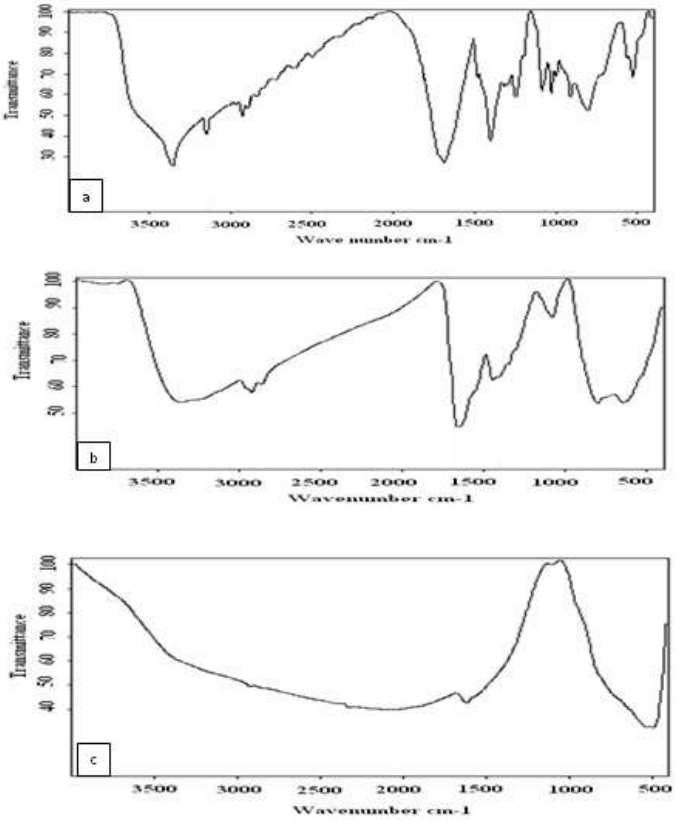


**Figure. 1. FTIR spectra of $TiO_2$ as prepared (a), calcined at 400° C(b), calcined at 500° C(c).**

### 3.2. XRD pattern of Nano Titania

The XRD pattern of the synthesized nano $TiO_2$ is shown in Fig (2). This study reveals that all the samples used in our investigation are crystalline in nature. The XRD patterns of the dried and calcined samples at 150 °C and 500$^oC$ clearly reveal that the phase transformation from the amorphous to the anatase state occurred at 500$^oC$.

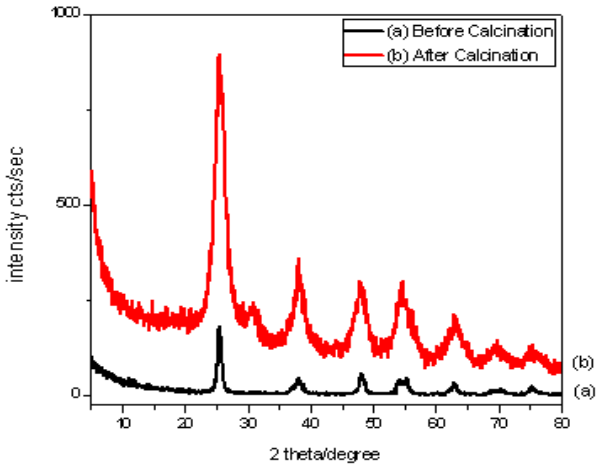


**Figure .2. XRD pattern of nano titania particles dried at 150° C(a) and calcined at 500° C (b)**

The crystalline size was estimated by the Scherer formula [34], which is generally the accepted method to estimate the mean crystalline size. The "d" spacing for the nano $TiO_2$ was 3.48nm and for Degussa P25, it was 3.52 nm. The XRD patterns exhibited strong diffraction peaks at 25.5°, 38.0° and 48.2°, indicating $TiO_2$ in the anatase phase. All the peaks are in good agreement with the standard spectrum (JCPDS no: 84-1286). Fig

(2) shows that the diffraction pattern peak intensity of $TiO_2$ increases with increasing particle size. No separate peak for the rutile phase was noticed. The peaks show that the $TiO_2$ sample has a single phase anatase structure. It has been observed that the peak broadening of (101) decreases with increasing calcination temperature. So, the calcination temperature plays an important role in controlling the crystallite size of $TiO_2$. The mole ratio of the starting materials chosen for the sample, indicates very fine and uniform nano $TiO_2$ particles. By controlling the acidity and the mole ratio of the starting materials, a nanosize particle can be obtained for anatase at 500°C.

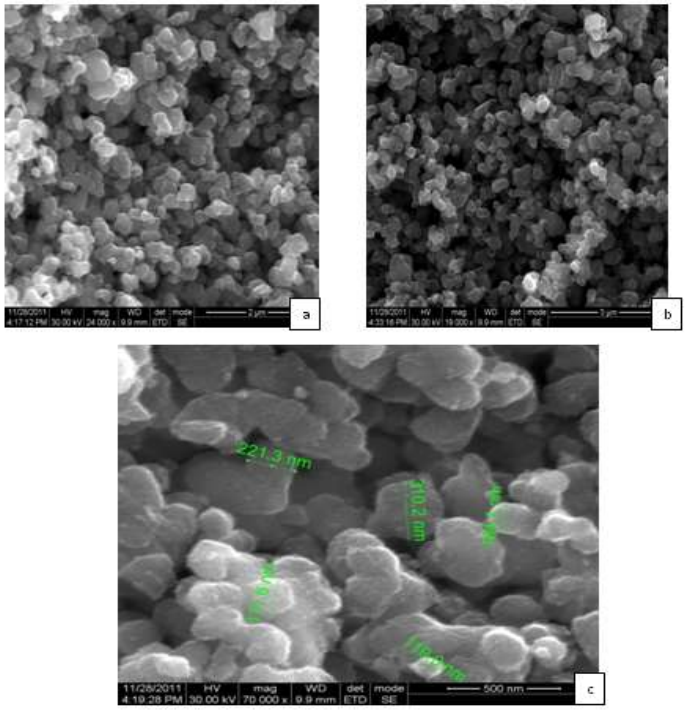


**Figure .3a, b, c SEM pictures of nano $TiO_2$ of different nanometers**

### 3.3. SEM images of Nano Titania

The morphology of the calcined Titania powders at 500 °C observed by the SEM and shown in Fig (3a,b,and c),are in the mole ratio of TTIP(1): EtOH(15): $H_2O$(60): HCl(0.2). The size of the Titania particles was uniform, and they were spherical in shape, constituted of sharp faceted nanocrystals. The result showed that the size of the catalyst was in the nanometer range, and the EDX picture Fig (4) also confirms the presence of the elements.

### 3.4. Thermo Gravimetric Analysis of Nano Titania

The thermal stability of theuncalcined and calcined Titania is represented in Fig (5).Thedesorption of the solvent and water was the reason for the 23% weight loss at 100°C on the catalyst surface. The second weight loss from 100°C to 470°C resulted from thestronger desorption of the organic solvent, which were trapped on the catalyst. At a higher temperature in the range of 500°C to 1000°C there was no weight loss.

### 3.5. Factors influencing the photocatalytic degradation

#### 3.5.1. The effects of the initial dye concentration on decolorization

It is important, both from a mechanistic and application point of view, to study the dependence of the photocatalytic reaction rate on the substrate concentration. It is generally noted that the degradation rate increases with an increase in the dye concentration up to a certain level, and tends to decrease with further increase in the dye concentration [35, 36]. The rate of degradation relates to the probability of the•OH radicals formation on the catalyst surface, and the probability of the•OH radicals reacting with the dye molecules. As the initial concentrations of the dye increase, the probability of the reaction between the dye molecules, and the oxidizing species also increases, leading to an enhancement in the decolorization rate. On the contrary, the degradation efficiency of the dye decreases as the dye concentration increases further. The presumed reason is that, at high dye concentrations the generation of the•OH radicals on the surface of the catalyst gets reduced, since the active sites are covered by the dye ions. Another possible cause for such results is the UV-screening effect of the dye itself. At a high dye concentration, a significant amount of UV may be absorbed by the dye molecules rather than bythe $TiO_2$ particles. This reduces the efficiency of the catalytic reaction, because the concentrations of •OH and $O_2$•− decrease [37-43].

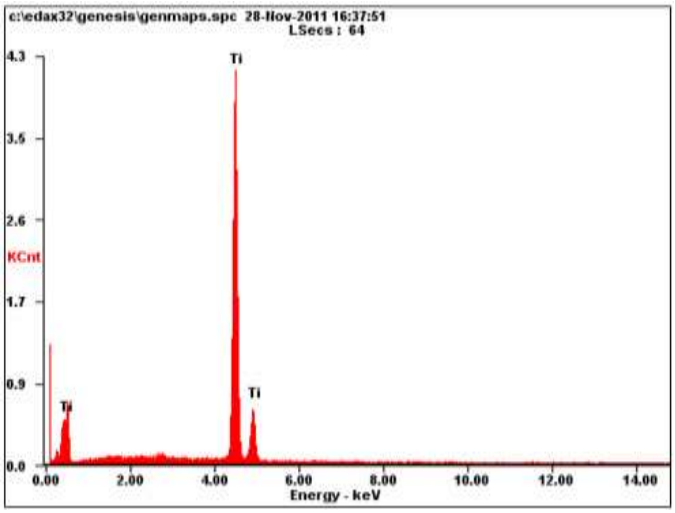


**Figure .4. EDX picture of nano $TiO_2$**

| Element | Weight | At% |
|---|---|---|
| CK | 23.49 | 55.05 |
| TiK | 76.51 | 44.95 |
| | | |

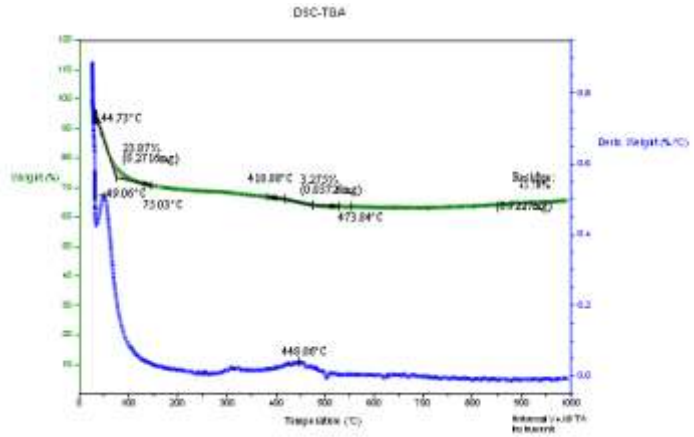


**Figure .5. TGA of as prepared and calcined Titania**

The effect of the initial concentration of the dye on the decolourisation rate was studied by varying the concentration from $1\times10^{-5}$ to $4\times10^{-5}$ M, with optimum catalyst loading. Then the rate of photocatalytic decolourisation was found to be the pseudo-first order kinetics, and the rate constant for this reaction was determined using the expression k=-2.303×slope. The plot of the normalized concentration of the dye versus irradiation

time, shows a good approximation over the range of $1\times10^{-5}$ to $4\times10^{-5}$ M of the dye concentration Fig 6, and its values are given in Table 1. The rate of photocatalytic degradation is found to decrease with further increase in the dye concentration. This may be attributed to the fact that the dye starts acting as a filter for the incident light,and does not permit the desired light intensity to reach the semiconductor surface in a limited time domain. Thus, a decrease in the rate of photocatalytic degradation of Rose bengal is observed at higher concentration.

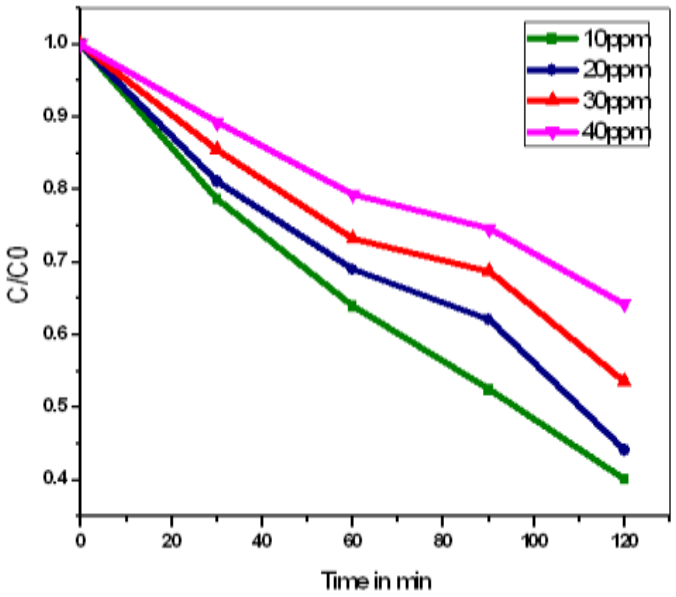


**Figure.6. Normalised Concentration of dye vs time for different concentration of dye with constant concentration of catalyst loading**

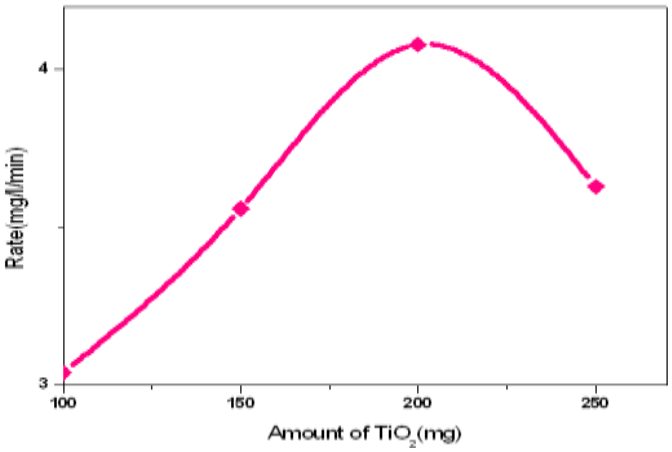


**Figure .7. Optimization of the weight of the catalyst ( different concentration of catalyst varying from 100mg/l to 250mg/l loaded with lower concentration of Rose bengal solution)**

### 3.5.2. Effect of catalyst concentrations

The results clearly show that increasing the amount of the catalyst from 100 mg to 200 mg increases the dye decolorization sharply from 37% to 60% for Rose bengal at 60 min. According to [44], the enhancement of the removal rate could be ascribed to:

- The increase in the amount of the catalyst weight, which increases the number of dye molecules adsorbed, and
- The density of particles in the area of illumination.

A series of experiments were carried out to assess the optimum catalyst loading, by varying the amount of the catalyst from 100 to 200 mg/100ml of the dye solution ($1\times10^{-5}$M). The rate constants of the dye degradation are presented in Table 2. It is seen that the rate constant increases linearly with catalyst loading up to 200mg/100ml. Above this (level of) catalyst loading, the increase in the turbidity of the solution reduces the light transmission through the solution,while below this level, it is assumed that the catalyst surface and absorption of light by the catalyst are limiting. The particle–particle interaction becomes significant as the number of particles in the solution increases. This reduces the site density of the surface holes and electrons [45]. The increased loading of the catalyst increases the quantity of photons adsorbed, and consequently increases the degradation rates. Hence, an optimum amount of the catalyst has to be added, in order to avoid unnecessary excess, and also to ensure the total absorption of light photons for efficient photo mineralisation[46] Fig 7. The corresponding UV spectra is shown in Fig 8 for 200 mg of catalyst loaded in a lower concentration of the dye solution .Other causes for this are an increased opacity of the suspension, brought about as a result of an excess of $TiO_2$ particles [47,48].Many authors have investigated the reaction rate as a function of catalyst loading under different experimental conditions [49, 50]. The results obtained in this work, are in good agreement with the reported values in the literature.

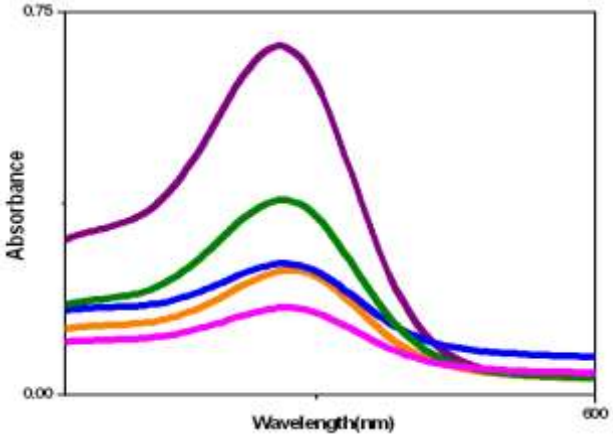


**Figure.8. UV spectra for Rose bengal dye solution of conc 1×10-5M loaded with 200mg/l catalyst**

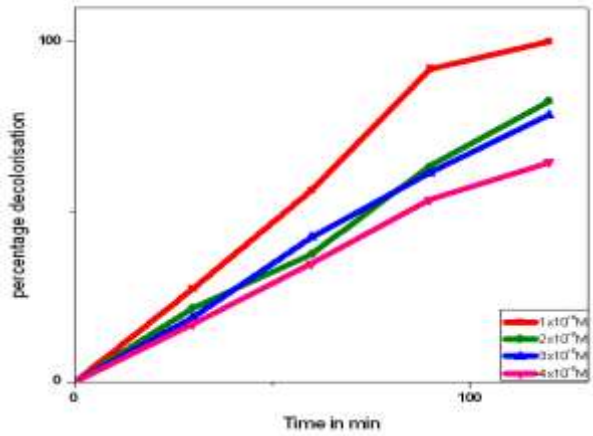


**Figure 9. Effect of concentration of dye on percentage decolourisation where different concentration of Rose bengal dye solution was loaded with 200mg/l of the Titania.**

### 3.5.3. Effect of the concentration of the dye on percentage decolourisation

The effect of the initial concentration of dyes on the percentage decolourisation was studied by varying the initial dye concentration from $1\times10^{-5}$ to $4\times10^{-5}$ M, with optimum catalyst loading shown in Fig 9. It can be seen from Table 3, that the

percentage decolourisation decreases on increasing the initial concentration of the dye. The possible explanation for this behaviour is that, as the initial concentration of the dye increases, the path length of the photons entering the solution decreases and at low concentrations, the reverse effect is observed;that is, an increase in the number of photon absorption by the catalyst, at lower concentrations[51].

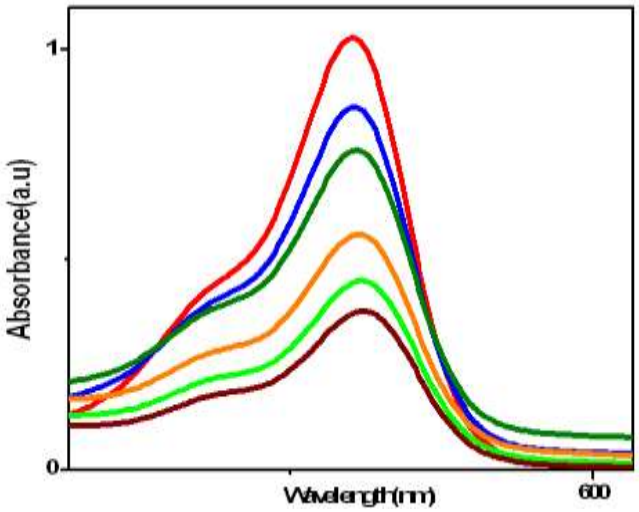


**Figure 10. Log of absorbance vs Time for lower conc of the dye shows the effect of irradiation time.**

### 3.5.4. Effect of irradiation time

The complete decolourisation of the dye occurred within 120 mins of irradiation, as shown in Fig 10. Table 4 represents the decolourisation of the dye at different irradiation periods at optimum catalyst loading, and dye concentration under experimental conditions. The photocatalytic decolourisation of the dye occurs on the surface of $TiO_2$, where the $OH^-$and $O_2$ radicals are trapped in the holes of the reactive species, as oxygen and water are essential for photocatalytic decolourisation. The $OH^-$radicals are strong enough to break the bonds in the dye molecules absorbed on the surface of $TiO_2$. When the intensity of light and dye concentration are constant, the number of $OH^-$ and $O_2$ radicals increases with an increase in the irradiation period, and hence, the dye molecules are completely decolorized.

**Effects of different catalysts and oxidising agents on the photodegradation of the dyes**

The effects of various photocatalyst, such as Degussa P-25, $TiO_2$ (anatase),and Photo Fenton reagent, on decolorization have been investigated at 100 mg/L catalyst concentration, $1\times10^{-5}$ to $4\times10^{-5}$ M dye concentrations at a pH of 3. The effect of the Fenton reagent with $TiO_2$ loading on Rose bengal dye for $1\times10^{-5}$ M is shown in Fig 11, and the normalised graph comparing the effect of the oxidising agent with other catalysts is shown in Fig 12.

In order to investigate the effect of $H_2O_2$ and $Fe^{2+}$ ion concentration on the decolourization efficiency, experiments were conducted at different $H_2O_2$ and $Fe^{2+}$ ion concentrations, and finally, for different concentrations of Rose bengal dye solution,2.5ml of $FeSO_4$ ($1\times10^{-3}$M), 0.5ml of $H_2O_2$ (30%). The effect of the Fenton reagent on $TiO_2$photo catalysis of Rosebengal is illustrated in Table 5. When a suitable amount of $Fe^{2+}/H_2O_2$ is present, reaction (1) becomes significant. When $Fe^{2+}/H_2O_2$ concentration is increased above the optimum concentration, the rate of photodegradation slowly decreases. However, as $Fe^{2+}/H_2O_2$ increases, the•OH produced from reaction (1) reacts with $H_2O_2$ more than before, thus producing $HO_2$• which can participate in the following reactions [52]:

$$Fe^{2+} + HO_2\bullet \rightarrow Fe(HO_2)^{2+} \quad (2)$$

$$Fe^{2+} + O_2\bullet^- + H^+ \rightarrow Fe(HO_2)^{2+} \quad (3)$$

$$Fe^{3+} + HO_2\bullet \rightarrow Fe^{2+} + O_2 + H^+ \quad (4)$$

$$Fe^{3+} + O_2\bullet^- \rightarrow Fe^{2+} + O_2 \quad (5)$$

Another reason for this negative effect due to the addition of more amount of Fenton reagent, is the formation of $Fe^{3+}$(reaction (1)) which initially forms complexes with both water and organic compounds [53, 54]. Hence, the active sites of the catalyst are covered with both $Fe^{2+}$and $Fe^{3+}$ions, and thus, the photon absorption by the catalyst decreases, and may affect •OH formation through the photocatalytic process on $TiO_2$. So, an optimum amount of $H_2O_2$ and $FeSO_4$ was determined. •OOH radicals are highly unstable in water and undergo facile disproportionate rather than reacting slowly with the dye molecules. The participation of the •OH radical as an active oxidizing species was confirmed [55]. The hydroxyl radical (oxidation potential 2.8 eV) attacks the dye, either byabstracting a hydrogen atom, or adding it to the double bonds. After continuous irradiation, the complete mineralization of the dye occurred via convertion into $CO_2$, $H_2O$, $NO_2^-$, $NO_3^-$, $SO_4^{2-}$[52, 53].The end products are simple molecules and harmless to the environment. (Eqn 6)

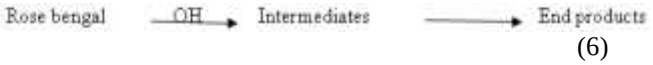


(6)

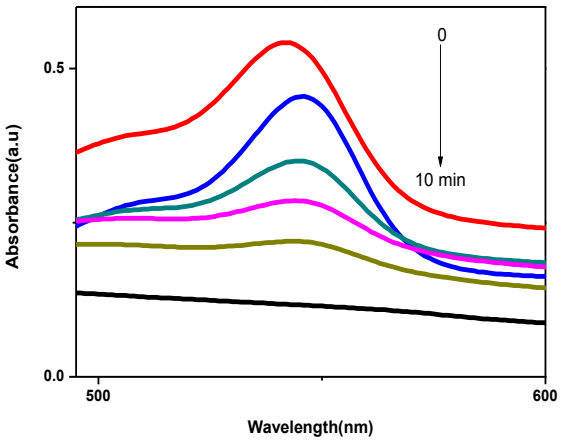


**Figure 11.Effect of $H_2O_2$ and $Fe^{2+}$ ions in $1\times10^{-5}$ M of Rose bengal with $TiO_2$ catalyst loading.**

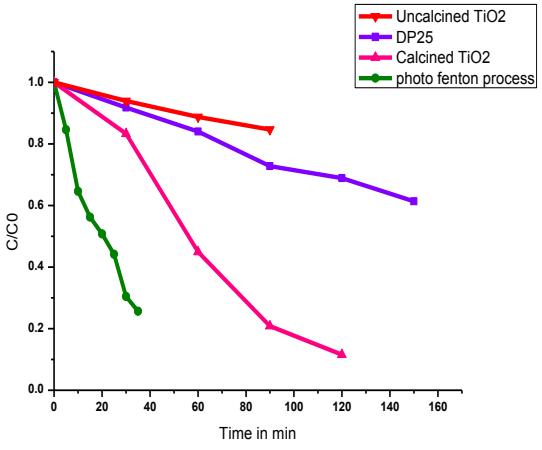


**Figure 12. The normalised graph comparing the effect of oxidising agent with other catalyst**

**Table 1: Effect of concentration of dye solution on the photocatalytic degradation. Dosage of Catalyst =200mg/100ml; Irradiation period= 2 h.**

| Time in min | Normalized Concentration | | | |
|---|---|---|---|---|
| | $1\times10^{-5}$M | $2\times10^{-5}$M | $3\times10^{-5}$M | $4\times10^{-5}$M |
| 0 | 1.000 | 1.000 | 1.000 | 1.000 |
| 30 | 0.787 | 0.811 | 0.855 | 0.892 |
| 60 | 0.639 | 0.690 | 0.733 | 0.793 |
| 90 | 0.524 | 0.621 | 0.688 | 0.746 |
| 120 | 0.401 | 0.442 | 0.536 | 0.642 |
| k'(min)-1 | 0.028 | 0.023 | 0.016 | 0.010 |
| Rate(mg/L/min) | 2.830 | 4.520 | 4.920 | 4.080 |

**Table 2: Effect of dosage of the catalyst on the photocatalytic degradation of dyes Concentration of the dye=$1\times10^{-5}$M; Irradiation period=150min**

| Amount of $TiO_2$(mg) | Rate(mg/L/min) |
|---|---|
| 100 | 3.04 |
| 150 | 3.56 |
| 200 | 4.08 |
| 250 | 3.68 |

**Table 3: Effect of concentration of dye solution on percentage decolourisation Irradiation period=120 min; Dosage of catalyst= 200mg/100ml**

| Time in min | Percentage Decolourisation | | | |
|---|---|---|---|---|
| | $1\times10^{-5}$M | $2\times10^{-5}$M | $3\times10^{-5}$M | $4\times10^{-5}$M |
| 0 | 0 | 0 | 0 | 0 |
| 30 | 27.3 | 21.6 | 19 | 16.9 |
| 60 | 56.3 | 37.5 | 42.5 | 34.7 |
| 90 | 92 | 63.4 | 61.4 | 53.5 |
| 120 | 100 | 82.6 | 78.4 | 64.6 |

**Table 4: Effect of irradiation period; Dye concentration=1×10-5M Amount of catalyst=200mg/100ml; pH=7**

| Time in min | % Decolourisation |
|---|---|
| 0 | 0 |
| 30 | 27.3 |
| 60 | 56.3 |
| 90 | 92 |
| 120 | 100 |

**Table 5: Effect of Fenton's reagent on $TiO_2$ on Rose bengal dye**

| Time in min | % Decolourisation (Using Fenton's Reagent) | Time in min | % Decolourisation (Using $TiO_2$) |
|---|---|---|---|
| 0 | 0 | 0 | 0 |
| 10 | 27.3 | 30 | 10.08 |
| 20 | 50.2 | 60 | 22.3 |
| 25 | 62.6 | 120 | 45.8 |
| 30 | 78.3 | 180 | 52.4 |
| 35 | 86 | 210 | 63.6 |
| 40 | 100 | 240 | 70.08 |

**Table 6: Kinetics constants for the decolourisation of Rose bengal using different process**

| Process | Rate constant(min-1) | $R^2$ |
|---|---|---|
| UV/Degussa P-25 | 0.0226 | 0.9293 |
| UV/Nano $TiO_2$ | 0.1141 | 0.98171 |
| Photo Fenton process | 0.3343 | 0.97963 |

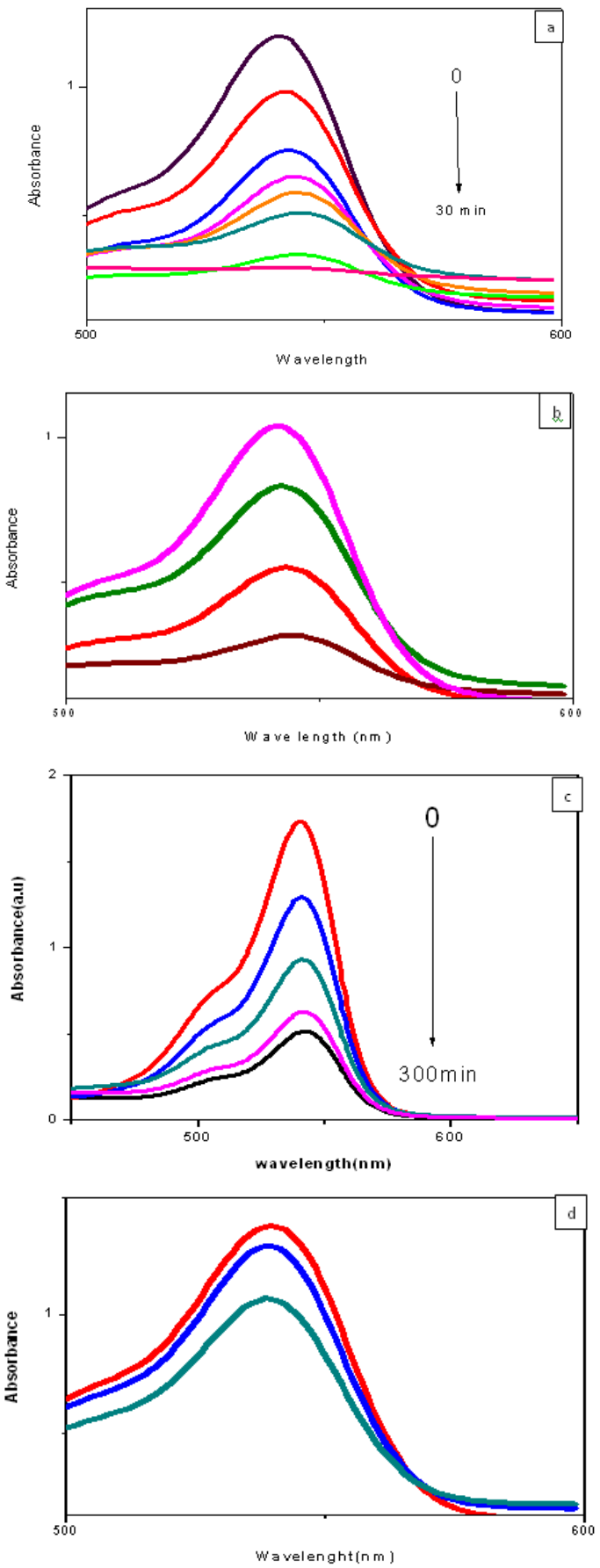


**Figure 13.UV-Vis spectra of Fentons reagent (a), Calcined Nano Titania (b), Degussa P-25 (c), Uncalcined Titania (d) loaded in Rose bengal dye solution ($4\times10^{-5}$M).**

Photo Fenton batch experiments were performed in a reactor with a reaction mixture of dye, $Fe^{2+}$, $H_2O_2$ and UV light source. The required amounts of $Fe^{2+}$ ions were added, and the pH was adjusted in optimum amounts of 3.0 with $H_2SO_4$, with the addition of $H_2O_2$ and UV light source, the Photo Fenton reaction is initiated. Continuous mixing was provided with a magnetic stirrer. The Fenton reagent is effective in decolorizing a wide range of dye [56,57]. Fenton's reagent works by oxidizing Ferrous to Ferric ion with the simultaneous splitting of $H_2O_2$ into hydroxide ion and hydroxyl radical [58]. The latter oxidizes the dye while the former precipitates ferric ion together with the organics. The reagent is used preferably at pH values around 3-4 [59-62]. From the results, the influence of the oxidising agents on the decolourization of the Rose bengal solution was illustrated, as seen in Fig (13a, b, c, d). In addition, the kinetic model, kinetic rates constant have been compared, and the rate constant of the Photo Fenton process was higher than the other processes given in Table 6.

**Conclusion**

Nano $TiO_2$ powders (Anatase form) were prepared using the sol-gel method of controlling the conditions properly. The photodegradation results showed that the degradation ofRosebengal was affected by the dyecatalyst concentrations and by theAdvanced Oxidation Process**.** The focus of the comparison of different AOPs methods was, to determine the best color removal performance, and the most efficient process for the removal of the target compound in the dye solution. The efficiency of the decolourization of the Rose bengal solution by different AOPs was illustrated. The most effective Rose bengal decolourization range was obtained by the Photo Fenton process, and the ranking was in the order of Photo Fenton >UV / Nano $TiO_2$> UV/ (DP-25). According to these results, clearly the rate constant of the Photo Fenton process was higher than that of the other processes. However, the selection of the suitable process for the treatment of pollutants was related to various conditions, such as theeconomical aspects, required equipments, operational problems, secondary pollutions, energy consumptions etc. The advantages of photo catalysis are: That it is destructive, there is no sludge production, and there is a potential of solar utilization. Fenton reaction waste water processes are known to be very effective in the removal of many hazardous organic pollutants from water, and have also been reported to achieve the degradation of organic compounds in a short period of time. The applications presented in this paper confirm the efficiency of $TiO_2$ photocatalytic oxidation, and of the Fenton processin water purification on a laboratory scale, and encourage the need to be developed on a large scale.

**References**

[1] Fibre2fashion, Chinese Dyestuff Industry Market Analysis (date visited - May 22, 2010) Available at: http://www.fibre2fashion.com/industry-article/24/2308/chinese-dyestuff-industry-market-analysis1.asp

[2] Konstantinou, I.K & Albanis, and T.A. TiO2 – assited photocatalytic degradation of azo dyes in aqueous solution: kinectic and mechanistic investigation (2004) .A review. Appl. Catal. B: Environ. 49(1): 1-14.

[3] Gonçalves M. S. T, Pinto E. M. S, Nkeonye. P, Oliveira A. M. F. -Campos. Degradation of C. I. Reactive Orange 4 and its Simulated Dyebath Wastewater by Heterogeneous Photocatalysis. (2005) Dyes and Pigments. 64: 135–139.

[4] Giwa.A, Ajibike M, Ismail A. Potentials of Calcium Hydroxide and Ferrous Sulphate in the Treatment of Textile Wastewater. (2007) A. J. of Nat. Sci. 10: 25–28.
[5] Rauf M. A, Ashraf S. S. Fundamental principles and application of heterogeneous photocatalytic degradation of dyes in solution. (2009) Chem. Eng. Jour. 151 : 10-18.
[6] Akpan U. G, Hameed B. H. Parameters affecting the photocatalytic degradation of dyes using $TiO_2$-based photocatalysts: (2009) A review. J of Hazard. Mater. 170: 520–529.
[7] Abbas M, Robab H. Ultrasonic degradation of Rhodamine B in the presence of $H_2O_2$ and some metal oxide. (2010) Ultrason. Sonochem. 17: 168–172.
[8] Mahamuni N. N, Adewuyi Y. G. (2010) Ultrason. Sonochem. 17:990.
[9] Arslan-Alaton I, Tureli G, Olmez-Hanci T. (2009) J. Photochem. Photobiol. A. 202: 142.
[10] Chen C. C, Ma W. H, Zhao J. C, (2010) Chem. Soc. Rev. 39: 4206.
[11] Akpan U. G, Hameed B. H. (2009) J. Hazard. Mater. 170: 520.
[12] Vinod Gopal K, Kamat P.V. Enhanced rates of photocatalytic degradation of an azo dye using $SnO_2$/$TiO_2$ coupled semiconductor thin films. (1995) Envorn. Sci. Technol. 29: 841.
[13] Neppolian B, Choi H. C, Sakthivel S, Arabindoo B, Murugesan V. Solar/UV-induced photocatalytic degradation of three commercial textile dyes. (2002) J. Hazard. Mater. B. 89: 303.
[14] Lathasree S, Nageswara R, Sivasankar B, Sadasivam V, Rengaraj K. Heterogeneous photocatalytic mineralization of phenols in aqueous solutions. (2004) J. Mole. Catal. A: Chem. 223: 101.
[15] Lizama C, Freer J, Baeza J, Mansilla H. D. Optimized photodegradation of Reactive Blue 19 on $TiO_2$ and ZnO suspensions. (2002) Catal. Today. 76:235.
[16] Akyol A, Yatmaz H. C, Bayramoglu M. Photocatalytic decolorization of Remazol Red RR in aqueous ZnO suspensions. (2004) Appl. Catal. B: Environ. 54: 19.
[17] Fujishima A, Zhang X, Tryk D. A. (2008) Surf. Sci. Rep. 63: 515.
[18] Chen X, Shen S, Guo L, Mao S. S. (2010) Chem. Rev. 110 : 6503.
[19] Moon S. J, So W. W, Park S. B, Kim K. J, Shin C. H. (2001) J. Mat. Sci. 36:4299.
[20] Lal M, Chhabra V, Ayyub P, Maitra A, (1988) J. Mater. Res. 13: 1249.
[21] Selvaraj U, Prasadrao A. V, Komerneni S, Roy R, (1992) J. Am. Ceram. Soc. 75: 1167.
[22] Fenton H. J. H. (1894) J. Chem. Soc. 65:899.
[23] Einsenhauer H. R. (1964) J. WPCF 36: 1117.
[24] Bishop D. F, Stern G, Fleisschman M, Marshall L. S. (1968) Ind. Eng. Chem. Dev. 7: 110.
[25] Barbeni M, Minero C, Pelizzetti E, Borgarello E, Serpone N. (1987) Chemosphere. 16: 2225.
[26] Walling C, (1975) ACC Chem. Res. 8: 125.
[27] Bigdha R. J. (1995) Chem. Eng.Prog. 12: 62.
[28] Nesheiwatt F. K, Swanson A. G. (2000) Chem. Eng. Prog. 96(4): 61.
[29] Grätzel C. K, Jirousek M, Grätzel M. (1990) J. Mol. Catal. 60: 375.
[30] Pelizzetti E, Carlin V, Minero C, Grätzel M. (1990) New J. Chem. 15: 351.
[31] Martin S. T, Lee A. T, Hoffmann M. R. (1995) Environ. Sci. Technol. 29: 2573.
[32] Sakthivel S, Neppolian B, Arabindoo B, Palanichamy M, Murugesan. V. (2000) Indian J. Eng. Mater. Sci. 7: 87.
[33] Sakthivel S, Neppolian B, Arabindoo B, Palanichamy M, Murugesan V. (2000) Indian J. Sci. Ind. Res. 59 : 556.
[34] Sakthivel S, Neppolian B, Arabindoo B, Palanichamy M, Murugesan V. (2001) Wat. Sci. Technol. 44(5): 211.
[35] Rush J. D, Bielski B. H. J. (1985) J. Phys. Chem. 89(23): 5062.
[36] Oliveros E, Legrini O, Hobl M, Muller T, Braun A. M. (1997) Chem. Eng. Proc. 36 : 397.
[37] Kwon B. G, Lee D. S, Kong N, Yoon N. (1999) Wat. Res. 33(9): 2110.
[38] Watts R. K, Bottenberg B. C, Hess T. F, Jensen M. D, Teel A. L. (1999) Environ. Sci. Technol. 33: 3432.
[39] Pirkanniemi K, Sillanpaa M. (2002) Chemosphere. 48: 1047-1060.
[40] Fujishima A, Rao T. N, Tryk D. A. (2000) J. Photochem. C1 1-21.
[41] Namboodri C. G, Walsh W. K. (1995) Am. Dyest. Rep. 84: 86.
[42] KuO W. G. (1992) Wat. Res. 26: 881.
[43] Lin S. H, Peng C. F. (1995) Environ. Technol. 16: 693.
[44] Wang C.C, Lee C.K, Lyu M.D, Juang L.C, Photocatalytic degradation of C.I. Basic Violet 10 using $TiO_2$ catalysts supported by Y zeolite: an investigation of the effects of operational parameters, (2008) Dyes and Pigments, 76 : 817–824.
[45] Cullity B.D. Adison-Wesley. (1978).
[46] Saquib M, Muneer M. (2003) Dyes and Pigments. 56: 37–49.
[47] Sakthivel S, Neppolian B, Shankar M. V, Arabindoo B, Palanichamy M, Murugesan V. (2003) Solar Energy Mater. Solar Cells. 77: 65.
[48] Tang W. Z, An H. (1995) Chemosphere. 31: 4157.
[49] So C. M, Cheng M. Y, Yu J. C, Wong P. K. (2002) Chemosphere. 46: 905.
[50] Grzechulska J, Morawski A. W. (2002) Appl. Catal. B: Environ. 36: 45.
[51] Daneshvar N, Salari D, Khataee A. R, (2003) J. Photochem. Photobiol. A: Chem. 157: 111.
[52] Reutergarth L. B, Iangphasuk M. (1997) Chemosphere. 35: 585.
[53] Mills A, Davis R. H, Worsley D. (1993) Chem. Soc. Rev. 22: 417.
[54] Poulios I, Aetopoulou I, (1999) Environ. Technol. 20: 479.
[55] Wang C. C, Lee C. K, Lyu M. D, Juang L. C. Photocatalytic degradation of C.I. Basic Violet 10 using $TiO_2$ catalysts supported by Y zeolite: an investigation of the effects of operational parameters. (2008) Dyes and Pigments. 76: 817–824.
[56] Lea J, Adesina A. A. (2001) J. Chem. Tech. Biotechnol. 76: 803-810.
[57] Herrmann J. M. (1995) Catal. Today. 24: 157-164.
[58] Moreira R. F. P. M, Sauer T, Cesconeto G, Jose H. J. (2002) J. Photochem. Photobiol. A. 149: 147-154.
[59] Lucas M. S, Peres J. A. (2006) Dyes and Pigments. 71: 236-244.

[60] Gouvea C. A, Wypych K. F, Moraes S. G, Duran N, Nagata N, Zamora P. P. Semiconductor-assisted photocatalytic degradation of reactive dyes in aqueous solution. (2000) Chemosphere. 40: 440-443.
[61] Saquib M, Muneer M. Semiconductor mediated photocatalyzed degradation of an anthraquinone dye, Remazol Brilliant Blue R under sunlight and artificial light source. (2000) Dyes and Pigments, 53: 237-249.
[62] Davis R. R. J, Gainer J. L, Neal G. P, Wewu I. (1994) Water Environment Res. 66 : 50.